Solid State Communications 150 (2010) 609–612

Contents lists available at ScienceDirect

Solid State Communications

journal homepage: www.elsevier.com/locate/ssc

# Electronic transport properties of the charge ordered manganite-based heterojunction

S. Liang *, J.R. Sun, Y.Z. Chen, W.M. Lv, B.G. Shen

*Institute of Physics and Beijing National Laboratory for Condensed Matter Physics, Chinese Academy of Sciences, Beijing 100190, People's Republic of China*

ARTICLE INFO

*Article history:*
Received 16 September 2009
Received in revised form
15 December 2009
Accepted 24 December 2009
by T. Kimura
Available online 4 January 2010

*Keywords:*
A. Manganite
A. Heterojunction
D. Charge order

ABSTRACT

The charge ordered $Bi_{0.4}Ca_{0.4}Sr_{0.2}MnO_3$ (BCSMO) film has been grown on (011) $SrTiO_3$: Nb (STON) (0.05 wt%) substrate. The charge ordering (CO) transition is realized at ∼336 K. The BCSMO/STON heterojunction shows excellent rectifying behavior. Through the capacitance measure of the junction, it is found that the built-in potential of the heterojunction is affected by the CO transition. A upward shift of the built-in potential of the junction appears around the CO transition temperature, which is ascribed to the change of the Fermi level in BCSMO film.

© 2010 Elsevier Ltd. All rights reserved.

## 1. Introduction

Perovskite manganites have attracted much attention in recent years because of their abundant properties associated with the strong coupling among the spin, charge and orbit degrees of freedom. In addition to colossal magnetoresistance, lots of physical phenomena have been observed in the manganites [1], such as the charge and orbital ordering, metal–insulator transition, phase separation, etc. Manganite-based heterojunctions also exhibit many interesting features, including excellent rectifying behavior, bias-dependent magnetoresistance, magnetic field tunable photovoltaic effects [2], and so on. A systematic study on manganite heterojunctions can give us not only the information on the interfacial properties of the strong electron-correlated oxides, but also excellent opportunities for the design and fabrication of the artificial devices with novel properties.

Generally, an energy barrier could be formed near the interface of the heterojunction, due to the difference of the Fermi energies of the two materials forming the junction. Based on the semiconductor theory, the change of band structure of the junction can affect the energy barrier. This has been verified for the conventional p–n junctions, whose properties can easily be tuned by dopant and an electric field. In manganites, it is found that the Fermi level can be controlled by the content of charge carriers [3,4]. So we can modulate the properties of manganite-based heterojunctions through changing the carrier density [5].

The bismuth-based manganite $Bi_{1-x}Ca_xMnO_3$ (BCMO) with a doping range from $x = 0.4$ to 0.82 [6,7] is a typical charge and orbital ordered manganite. The charge ordering (CO) transition in $Bi_{1-x}Ca_xMnO_3$ takes place against a paramagnetic (PM) background. Due to the lone pair $6s^2$ electron of $Bi^{3+}$, the CO transition temperature $T_{CO}$ is much higher than other manganites such as $Nd_{0.5}Sr_{0.5}MnO_3$ and $Pr_{0.5}Ca_{0.5}MnO_3$. When the BCMO is fabricated into film, the transition temperature $T_{CO}$ is lowered, due to the lattice strain in the film [7,8]. In the $Ln_{1-x}A_xMnO_3$ compounds, the $T_{CO}$ can be adjusted by tuning the one electron bandwidth [9]. A wide $e_g$ bandwidth, which appears when the mean ionic radius of the A-site cations is large, favors a low $T_{CO}$ due to the well itinerant character of the $e_g$ electrons, whereas a narrow bandwidth enhances the CO state. However, the bismuth-doped manganites do not exhibit this dependency, and the introduction of large ions sometimes causes a increase of the CO transition temperature. For example, the $T_{CO}$ in $Bi_{1-x}Sr_xMnO_3$ is generally higher than in $Bi_{1-x}Ca_xMnO_3$. A mechanism based on the manifestation of a $Bi^{3+}$ lone pair $6s^2$ character is proposed to justify the strong tendency of the charges to localizing and ordering [10]. In this paper, through tuning the concentration of $Sr^{2+}$ replacing $Ca^{2+}$ ions, the $T_{CO}$ of $Bi_{0.4}Ca_{0.4}Sr_{0.2}MnO_3$ film is tuned to ∼336 K, slightly above room temperature. This allows easy access of the built-in potential across the CO transition by various techniques such as the capacitance–voltage ($C$–$V$) and current–voltage ($J$–$V$) characteristics analysis. An obvious change of built-in potential resulted from the charge ordering is observed by the analysis of the $C$–$V$ relation.

## 2. Experiments

A ceramic target with the nominal composition of $Bi_{0.4}Ca_{0.4}Sr_{0.2}MnO_3$ (BCSMO) was prepared by a solid-state reac-

* Corresponding author. Tel.: +86 10 82648085; fax: +86 10 82649485.
*E-mail address:* liangshuo@g203.iphy.ac.cn (S. Liang).

0038-1098/$ – see front matter © 2010 Elsevier Ltd. All rights reserved.
doi:10.1016/j.ssc.2009.12.037

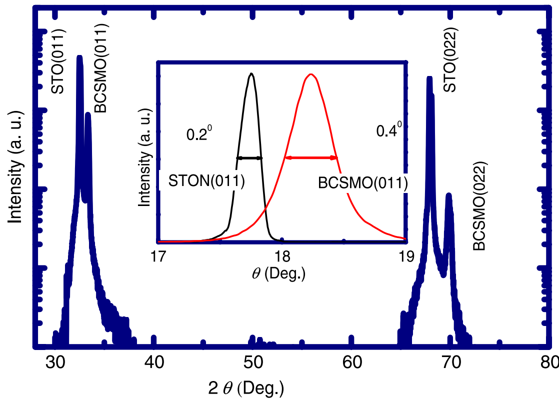


**Fig. 1.** XRD spectrum of the BCSMO film. The inset contains the rocking curves of (011) peak of BCSMO and STO.

tion. BCSMO film was grown on (011)-oriented $SrTiO_3$ : Nb (0.05 wt.%) (STON) substrates by the pulsed laser deposition method using a KrF excimer laser ($\lambda = 248$ nm). During deposition, the temperature of the substrate and the oxygen pressure in the chamber were kept at 700 °C and 60 Pa, respectively. The thickness of film is ∼180 nm, determined by the deposition time.

## 3. Results and discussion

X-ray diffraction (XRD) results of the BCSMO film are shown in the Fig. 1. The scanning range of $2\theta$ changes from 20° to 80°, and there is only the (011) and (022) peaks of BCSMO and STO. The FWHM of (011) peaks of BCSMO and STO are 0.4° and 0.2°, as shown in the inset of Fig. 1. The XRD results confirm the epitaxial growth of the BCSMO film. The distance between the {011} planes $d_{011}$ is ∼0.268 nm.

Transport and magnetic measurements were performed on a superconducting quantum interference device magnetometer (MPMS-7) equipped with an electric measure unit. Fig. 2 presents the temperature dependence of the magnetization ($M$) and resistivity ($\rho$) of the BCSMO film. The magnetization was recorded under the field of 4 T, with the contributions of the substrate being subtracted. With the increase of temperature, the magnetization of the film first decreases, becoming smallest at ∼286 K, then rises to a peak value at around 336 K. The film insulating over the whole temperature range is investigated. The obvious change on the $\rho$–$T$ curve appears at ∼336 K, where the magnetization peak on the $M$–$T$ curve shows up. In the inset of Fig. 2(b), the $d(\mathrm{Ln}\rho)/dT$–$T$ plot starts to become flat at ∼286 K and drops to a max value at ∼336 K with the increase of temperature. These features are the signature of the charge ordering transition, which sets in at ∼286 K and finishes at ∼336 K. The transition temperature is ∼40 K lower than it is in bulk. The shaded area in the inset of Fig. 2(b) expresses the CO transition degree [11,12].

The electronic transport properties of the BCSMO/STON junction are further studied. Focuses are the effect of the CO transition. Ag pads were deposited on BCSMO and STON, as electrodes. The electric contacts are proved to be Ohmic. The junction area is $1 \times 1$ mm$^2$. The temperature-dependent current–voltage characteristics of the BCSMO/STON junction are presented in Fig. 3. The junction shows an excellent rectifying behavior, as demonstrated by the strong asymmetry of the $J$–$V$ curves against the polarity of the electric bias in Fig. 3(a). The value of $J$ is negligible small in the negative direction up to the bias voltage 5 V, while it rises quickly in the positive direction when the bias voltage exceeds a threshold value below 1 V. As the temperature increases, the $J$–$V$ curves shift along the $V$ axis to the low bias voltage direction. In other manganite junctions, the rectifying behavior has also been reported, except for the difference of threshold voltage.

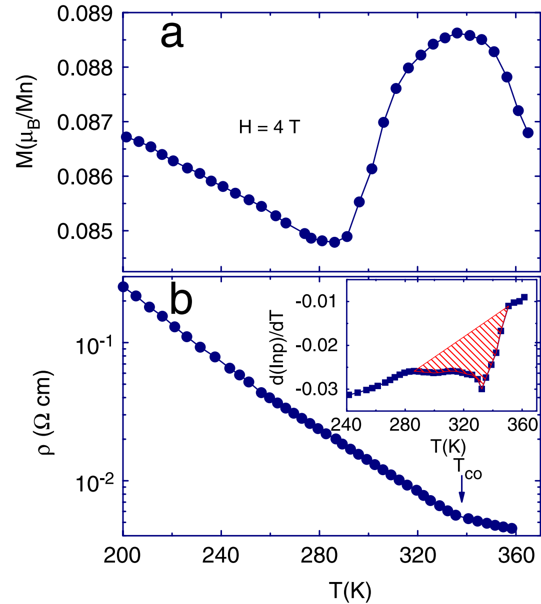


**Fig. 2.** (a) The temperature dependence of the magnetization of the BCSMO film. (b) The temperature dependence of the resistivity of the BCSMO film. The inset of (b) is the $d(Ln\rho)/dT$–$T$ plot of BCSMO film. The shaded area expresses the CO transition degree.

To obtain the information of the interfacial potential, the $J$–$V$ curves have been further analyzed. Based on the semiconductor theory, the $J$–$V$ relation can be described by the formula $J \approx J_s \exp(qV/nk_BT)$ in the positive bias direction when $qV \gg nk_BT$, where $J_s$ is the saturation current, $k_B$ the Boltzmann constant, and $n$ the ideality factor. The value of $n$ changes from ∼1.1 to 1.16 in the investigated temperature range, as shown in the upper inset of Fig. 3(a). This indicates that the thermal current is dominative in the junction. The saturation current, which varies exponentially against the interfacial barrier, can be obtained as the intercept in the $J$ axis of the extrapolated $\log J$–$V$ curve. Fig. 3(b) is the $\log J$–$V$ plots for the selected temperatures from 300 K to 400 K. Well linear $\log J$–$V$ relations are observed for all the temperatures in a wide bias range. The nonlinearity in the high bias range could be ascribed to the effect of the contact resistance, which becomes important under a high bias voltage. The Schottky barrier height (SBH) $\Phi_B$, which is the difference of the Fermi level of BCSMO and the bottom of the conduction band of STON, can be derived from $J_s$ based on the relation $J_s \propto A^*T^2 \exp(q\Phi_B/k_BT)$, where $A^*$ is the Richardson's constant. In the bottom inset of Fig. 3(a), the $\mathrm{Ln}(J_s/T^2)$–$1/T$ plot is presented. The slope of the plot is almost a constant at the investigated temperature region, and $\Phi_B = 1$ V is calculated from the slope. It indicates that there is no obvious response of $\Phi_B$ to a charge ordering transition at ∼336 K. Similar results have been obtained in $Nd_{0.5}Sr_{0.5}MnO_3$/STON and $La_{0.875}Sr_{0.125}MnO_3$/STON junctions [13,14], although the $Nd_{0.5}Sr_{0.5}MnO_3$ and $La_{0.875}Sr_{0.125}MnO_3$ films experience clear CO transition. This may be ascribed to either the spatial inhomogeneity of the interfacial barrier, or the appearance of the interface state [15].

The capacitance–voltage ($C$–$V$) relation of the junction can also give the information of the interfacial energy barrier. The capacitance of a Schottky junction obeys the relation of $1/C^2 = 2(V_{bi} - V)/q\varepsilon_{STON}N_{STON}$, where $N_{STON}$ is the Nb-dopant concentration, $\varepsilon_{STON}$ the permittivity of STON, and $V_{bi}$ the built-in potential. The capacitance of the BCSMO/STON junction under different negative bias voltages is measured in the temperature range from 300 K to 400 K. Fig. 4(a) shows the $1/C^2$–$V$ characteristics of the junction. A linear behavior of the $1/C^2$–$V$

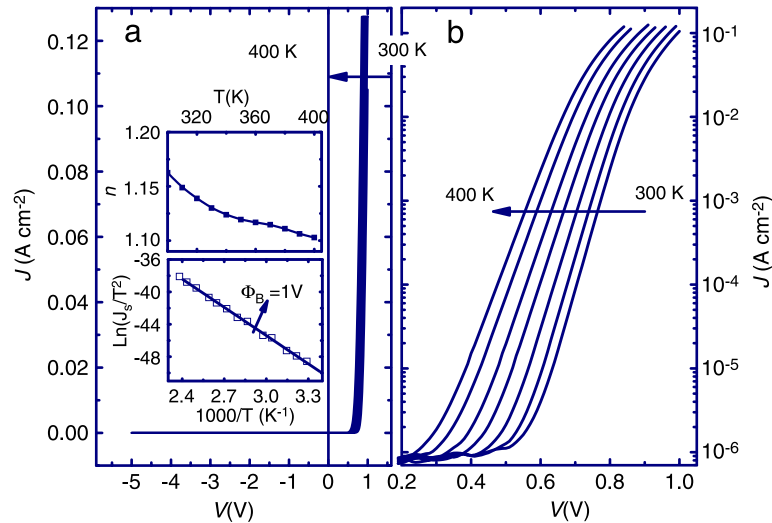


**Fig. 3.** Linear (a) and semilog (b) of the $J$–$V$ characteristics of BCSMO/STON measured from 300 K to 400 K. The insets are the temperature-dependent ideality factor $n$ and the Ln($J_s/T^2$)–$1/T$ plot. The solid line is a guide for the eye.

plot is observed. The temperature dependence of $V_{bi}$ shown in the Fig. 4(b) is obtained from the intersection of the straight fitting lines with the $V$ axis. With the decrease of temperature, the $V_{bi}$–$T$ relation shows a upward shift at ∼340 K, around $T_{CO}$. Given the nearly linear temperature dependence of $V_{bi}$ above $T_{CO}$, we extrapolating the data of $V_{bi}$ above $T_{CO}$ to 300 K. As shown in the inset of Fig. 4(b), the difference between the $V_{bi}$ in CO state and the extrapolating data, $\Delta V_{bi}$, begins to increase at ∼340 K, develops with the decrease of temperature, and saturates below ∼280 K. This is exactly the temperature range for the emergence and development of the charge ordering as shown in Fig. 2. Since the band structure of STON is nearly independent of temperature, the data in Fig. 4 suggest that the CO transition in BCSMO affects the electronic structure of the junction.

The value of $V_{bi}$ is larger than the results before [5,14]. It is suggested that the tunneling current, spatial barrier inhomogeneities or the interface state between the metal and semiconductor may reduce the capacity of junction and enhance $V_{bi}$. Fortunately, the interfacial state does not blur the effect of the CO on $V_{bi}$ [15].

Considering that the Fermi level of STON is near the conduction band bottom [16], the $V_{bi}$ of BCSMO/STON junction approximately equals the height of Schottky barrier. The upward shift of $V_{bi}$ around $T_{CO}$ indicates that the Fermi level of the BCSMO film is turned down by the CO transition. Generally, the appearance of a charge ordering state is always accompanied by the opening of the band gap near the Fermi level, which is due to the Coulomb repulsion [14,17]. The $\Delta V_{bi}$, as we discussed above, should quantify the CO gap. The appearance of a CO gap would cause the shift of the Fermi level. On the other side, the Fermi level is related to the carrier density. According to the results in the $Bi_{0.4}Ca_{0.6}MnO_3$ film [8], the carrier density decreases exponentially with the temperature below $T_{CO}$, which may indicate a reduction of the Fermi level. A clear upward shift of $V_{bi}$ also appears in the $La_{0.875}Sr_{0.125}MnO_3$(LSMO)/ STON heterojunction [14] when the CO transition occurs. However, in the BCSMO/STON junction, the film transits into the CO state from the PM insulating state instead of the metallic one in the LSMO film.

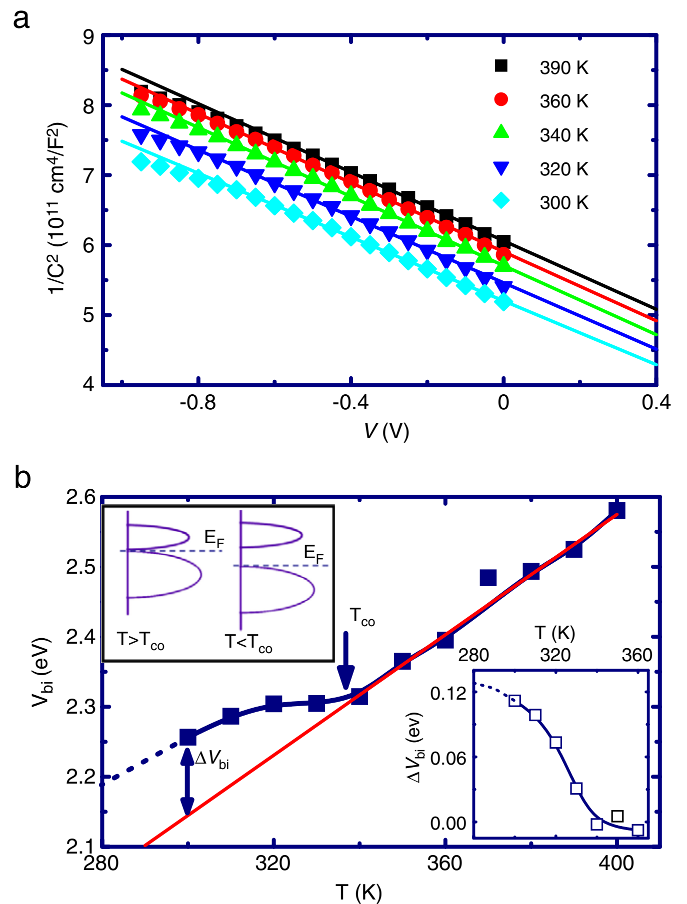


**Fig. 4.** (a) The $1/C^2$–$V$ characteristics of BCSMO/STON from 300 K to 400 K. (b) The temperature dependence of $V_{bi}$. The inset contains the schematic Fermi-level shift in BCSMO induced by the CO transition (upper), and the temperature-dependent $\Delta V_{bi}$ (lower).

## 4. Conclusions

The BCSMO film has been grown on a (011) STON substrate and the CO transition is realized at 336 K, which is verified by the magnetic and transport properties. The BCSMO/STON heterojunction shows excellent rectifying behavior. Through the capacitance measure of the junction, it is found that the CO transition affects the built-in potential, thus the SBH of the heterojunction. With the decrease of temperature, the $V_{bi}$ drops and shows an upward shift of around $T_{CO}$. This is ascribed to the shift of the Fermi level in the BCSMO film.

## Acknowledgement

This work has been supported by the National Natural Science Foundation of China and the State Key Project for the Fundamental Research of China.

## References

[1] For a review, see Y. Tokura (Ed.), Colossal Magnetoresistive Oxides, Gordon and Breach, New York, 2000.
[2] J.R. Sun, C.M. Xiong, T.Y. Zhao, S.Y. Zhang, Y.F. Chen, B.G. Shen, Appl. Phys. Lett. 84 (2004) 1528;
J.R. Sun, C.M. Xiong, Y.F. Chen, B.G. Shen, L. Kang, Europhys. Lett. 66 (2004) 868;
Z.G. Sheng, B.C. Zhao, W.H. Song, Y.P. Sun, J.R. Sun, B.G. Shen, Appl. Phys. Lett. 87 (2006) 242501.
[3] J.H. Park, C.T. Chen, S.W. Cheong, W. Bao, G. Meigs, V. Chakarian, Y.U. Idzerda, Phys. Rev. Lett. 76 (1996) 4215.
[4] K. Ebata, H. Wadati, M. Takizawa, A. Fujimori, A. Chikamatsu, H. Kumigashira, M. Oshima, Y. Tomioka, Y. Tokura, Phys. Rev. B 74 (2006) 064419.
[5] W.M. Lü, J.R. Sun, D.J. Wang, Y.W. Xie, S. Liang, Y.Z. Chen, B.G. Shen, Appl. Phys. Lett. 92 (2008) 062503.
[6] W. Bao, J.D. Axe, C.H. Chen, S.W. Cheong, Phys. Rev. Lett. 78 (1997) 543.
[7] H. Woo, T.A. Tyson, M. Croft, S.W. Cheong, J.C. Woicik, Phys. Rev. B 63 (2001) 134412.
[8] Y.Z. Chen, J.R. Sun, D.J. Wang, S. Liang, B.G. Shen, J. Phys.: Condens. Matter 19 (2007) 442001.
[9] C.N.R. Rao, A. Arulraj, P.N. Santosh, A.K. Cheetham, Chem. Mater. 10 (1998) 2714.
[10] J.L. Garcıa-Munoz, C. Frontera, M.A.G. Aranda, A. Llobet, C. Ritter, Phys. Rev. B 63 (2001) 064415.
[11] Y.Z. Chen, J.R. Sun, S. Liang, W.M. Lv, B.G. Shen, W.B. Wu, J. Appl. Phys. 103 (2008) 096105.
[12] J.Z. Wang, J.R. Sun, W. Zhang, R.C. Yu, Y.Z. Chen, B.G. Shen, W.B. Wu, Europhys. Lett. 82 (2008) 16002.
[13] J. Matsuno, A. Sawa, M. Kawasaki, Y. Tokura, Appl. Phys. Lett. 92 (2008) 122104.
[14] Y.Z. Chen, J.R. Sun, A.D. Wei, W.M. Lu, S. Liang, B.G. Shen, Appl. Phys. Lett. 93 (2008) 152515.
[15] Y. Hikita, Y. Kozuka, T. Susaki, H. Takagi, H.Y. Hwang, Appl. Phys. Lett. 90 (2007) 143507.
[16] B. Stoeckly, Appl. Phys. Lett. 36 (1980) 384.
[17] A. Biswas, A.K. Raychaudhuri, R. Mahendiran, A. Guha, R. Mahesh, C.N.R. Rao, J. Phys.: Condens. Matter 9 (1997) L355.